Dual Chemical-Electric Propulsion Systems Design for Interplanetary CubeSats

Mani, Karthik Venkatesh; Topputo, Francesco; Cervone, Angelo

Publication date
2018

Document Version
Accepted author manuscript

Published in
ESA Space Propulsion 2018 Conference, Seville, Spain

DUAL CHEMICAL-ELECTRIC PROPULSION SYSTEMS DESIGN FOR INTERPLANETARY CUBESATS

Karthik Venkatesh Mani[(1)], **Francesco Topputo**[(1)], **Angelo Cervone**[(2)],

[(1)] *Politecnico di Milano, Italy, karthikvenkatesh.mani@polimi.it*

[(1)] *Politecnico di Milano, Italy, francesco.topputo@polimi.it*

[(2)] *Delft University of Technology, the Netherlands, a.cervone@tudelft.nl*

KEYWORDS: Interplanetary CubeSat Propulsion

ABSTRACT

Interplanetary CubeSats enable universities and small-spacecraft-consortia to pursue low-cost, high-risk and high-gain Solar System Exploration missions, especially Mars; for which cost-effective, reliable, and flexible space systems need to be developed. Missions to Mars can be achieved through a) in-situ deployment by a mothership and b) highly flexible stand-alone CubeSats on deep-space cruise. The current work focuses on sizing and establishing critical design parameters for *dual* chemical-electric propulsion systems that shall enable a stand-alone 16U CubeSat mission on a hybrid high-thrust & low-thrust trajectory. High thrust is used to escape Earth whereas low-thrust is used in autonomous deep-space cruise, achieving ballistic capture, and emplacement on an areosynchronous orbit at Mars. Chemical propulsion characterisation is based on ΔV requirement and a heuristic optimisation of thrust, specific impulse and burn time while balancing transfer time and propellant mass. Limitations are set to minimise destabilising momentum. Electric propulsion characterisation is based on the ΔV, power consumption, and trajectory requirements for fuel-optimal and time-optimal strategies. The sizes amount to $\sim 16\%$ and $\sim 21\%$ of the assumed total mass (~ 30 kg) for chemical and electric systems, respectively.

1. INTRODUCTION

CubeSats have been in usage for Earth-based missions since the turn of the century for multifarious applications including Earth-observation, climate assessment, lower thermosphere characterisation, and biological research etc [1]. Development of such CubeSats have primarily been pursued by Universities and small-spacecraft-consortia. Present-day CubeSats have a size range between 1U to 6U, and they do not have primary propulsion systems to perform critical orbital manoeuvres as they are designed to maximise payload performance and operate for a short duration. Only two CubeSat missions have done a technology demonstration of propulsion systems, albeit with limited capability. The IMPACT mission utilised several electrospray thrusters and the BricSAT-P utilisied 4 microcathode arc thrusters [2]. Predominantly, CubeSat *propulsion* pertains to the usage of systems for attitude control, station-keeping, and reaction wheel desaturation [3].

To expand the horizons, Interplanetary CubeSats development will be a necessary step for increasing the solar system exploration efforts at high science-to-investment ratio. Interplanetary CubeSats design and development shall push the frontiers of engineering and technology by the means of miniaturising and simultaneously increasing the functionality of critical space systems. Improvements are envisaged in the fields of long-distance communications, deep-space autonomous guidance-navigation-control, propulsion for trajectory control, accurate ADCS, and high-speed low-power on-board data processing [4].

Missions to Mars could be achieved through a) in-situ deployment by a mothership and b) highly flexible stand-alone CubeSats on deep-space cruise. Stand-alone CubeSats to Near-Earth Objects have been shown to be feasible, such as the M-ARGO mission by ESA [5]. Owing to communications and power production limitations, M-ARGO study revealed that the limit region reachable by a CubeSat is 1.2 to 1.3 AU. Improvements to communication, power, and propulsion systems could push the envelope to 1.5 AU, thereby making a stand-alone Mars CubeSat feasible. NASA's Mars Cube One (MarCO) mission [6, 7], which is yet to be launched, is a two 6U CubeSat segment mission that is deployed in-situ by the SLS launch vehicle alongside the InSight lander mission to Mars. These two 6U CubeSats provide communications relay and support during Mars atmospheric entry.

Stand-alone Interplanetary CubeSat missions from Earth to Mars require robust primary propulsion for precise trajectory control and orbital manoeuvring that shall increase their flexibility and autonomy. The main motivation for this work is the need for development of propulsion systems that enable interplanetary CubeSat missions. A successful design, implementation, and proof of concept of on-board

propulsion systems shall revolutionise the future missions and the capabilities of CubeSats to perform critical missions beyond LEO will drastically increase. On-board propulsion also broadens the launch windows and the launch could be shared with any primary payload that is bound for a high-energy Earth orbit, for example, Supersynchronous Geostationary Transfer Orbit (SSGTO) as the frequency of such lauches is high ($\sim$ 10 per year). In contrast, Earth escape launches occur only 1-2 times a year.

To this extent, the **M**ars **A**tmospheric **R**adiation **I**maging **O**rbiter (MARIO) mission is studied. The mission is envisaged to be launched into a high-energy geocentric orbit, perform orbit raising and Earth escape, cruise in deep-space, achieve ballistic capture at Mars [8], and enter an areosynchronous orbit. The mission statement:

> *The Mars Atmospheric Radiation Imaging Orbiter (MARIO) is a stand-alone CubeSat exploration mission to Mars that shall demonstrate the capabilities of CubeSats to escape Earth, perform autonomous deep-space cruise, achieve ballistic capture, and be emplaced on an areosynchronous orbit at Mars. It shall utilise dual chemical-electric propulsion, concomitant with hybrid high-thrust low-thrust trajectories and autonomous GNC. The MARIO mission shall conduct radiation imaging to characterise the thermal environment in the Mars upper atmosphere. The mission shall serve as a pioneer for Interplanetary CubeSat missions with high launch flexibility and cost efficiency.*

This work pertains to the delineation of sizing and design parameters of the propulsion systems that shall enable the MARIO mission. Dual chemical-electric propulsion is used, wherein the chemical stage enables orbit raising and Earth escape while the electric stage enables deep-space cruise and ballistic capture.

Owing to the significant increase in the CubeSats development and the efforts to increase their capabilities, multiple propulsion systems are currently being developed. Although, much of the information is not available publicly. Chemical propulsion systems applicable to Interplanetary CubeSats include monopropellant thrusters [9, 10], bipropellant thrusters [11], tripropellant [12], cold gas [2, 6, 13], warm gas [14], solid [15] and hybrid motor systems [16]. These systems have been manufactured and tested on-board large satellites but they face multiple issues over miniaturisation [17]. The Monopropellant and Bipropellant systems are the most suitable for stand-alone Interplanetary CubeSat chemical propulsion module due to their high performance characteristics [13]. Electric propulsion systems for CubeSat applications include electrostatic thrusters like Gridded Ion Thrusters [18, 19], Hall Thrusters [20, 21] and Field Emission Electric Propulsion [22]; electromagnetic thrusters like Pulsed Plasma Thrusters [23], Magnetoplasmadynamic Thrusters [24] and Helicon Thrusters [25, 26]; and electrothermal thrusters like Resistojets [27] and Arcjets [28]. Owing to high specific impulse requirements and long mission lifetime, Gridded Ion Thrusters fit the bill for Interplanetary CubeSats on deep-space cruise [13, 29].

In this work, Section 2 delineates the mission characteristics of MARIO and the dual propulsion concept. In Section 3, the main considerations of the chemical propulsion design are first highlighted, mission analysis for Earth escape phase is done, desired performance parameters like thrust, specific impulse and firing times are calculated, and the sizing is performed. In Section 4, candidate electric propulsion systems are highlighted and a preliminary trade-off is performed. Thruster characteristics are highlighted and an optimal control problem is solved to compute the trajectory, overall ΔV, and the required propellant mass. Finally, the system sizing is performed. Section 5 highlights the characteristics of the combined chemical-electric propulsion systems.

2. MISSION CHARACTERISTICS

In accordance with MARIO's mission statement, the stand-alone CubeSat shall escape Earth, through multiple orbit raising manoeuvres starting from a high-energy supersynchronous elliptical geostationary transfer orbit with a perigee of 295 km and an apogee of 90,000 km that is used for some communication satellites. Falcon 9 v1.1 rocket launched SES-8 in December 2013 and Thaicom 6 in January 2014 into this orbit [30]. Owing to the frequency of communication satellite launches ($\sim$ 10 per year), this high-energy orbit was selected to a) improve the launch opportunities and widen the launch window and b) reduce the ΔV required for Earth escape. Owing to the presence of Van Allen radiation belts and the expected multiple crossings of the spacecraft during orbit raising, it is prudent to embark on an escape trajectory swiftly to reduce radiation damage. Thus, a high-thrust chemical propulsion system is required to provide high ΔV within a short duration since a low-thrust electric propulsion system will drastically increase the residence time of the spacecraft in the radiation belts. Per contra, CubeSats cannot handle very high thrusts due to the possibility of irrecoverable destabilising angular momentum caused by the thrust misalignment. Moreover, the limitation on the maximum thrust leads to a longer burn time of the thruster. Long burn times with limited thrust lead to gravity losses [32]. Thus, the chemical propulsion system needs to fire for a specific duration with a specific thrust such that a) swift escape is achieved and b) gravity loss and undesired destabilising momentum are minimised. Fig. 1a illustrates the orbit raising and escape using chemical propulsion.

Once Earth escape is achieved, the chemical propulsion is extinguished and the Low-Thrust Deep-Space Cruise phase starts as the spacecraft is now in heliocentric orbit (Fig. 1b). The spacecraft utilises the novel autonomous optical navigation technique [33] while on deep-space cruise and full-disk optical navigation while nearing Mars [34]. The electric propulsion system, which has very high specific impulse, is utilised during this phase. The required ΔV for reaching Mars is accumulated over the long transfer period. Two

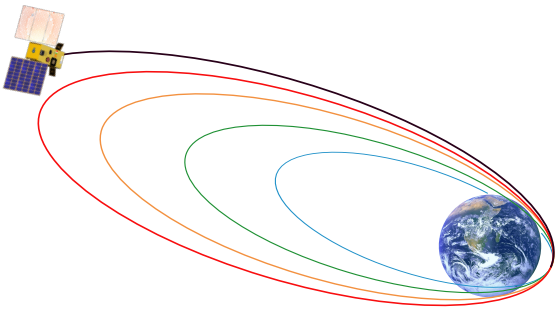

(a) Orbit raising manoeuvres using chemical propulsion to achieve Earth escape.

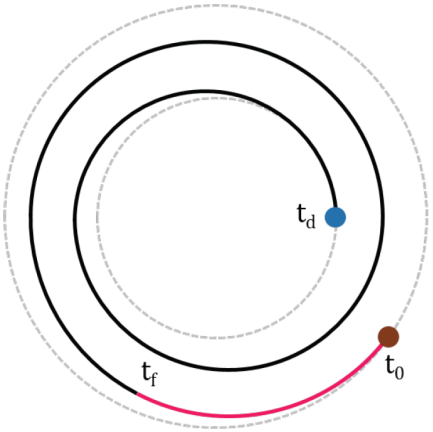

(b) Deep-space cruise and ballistic capture. Image source [31]

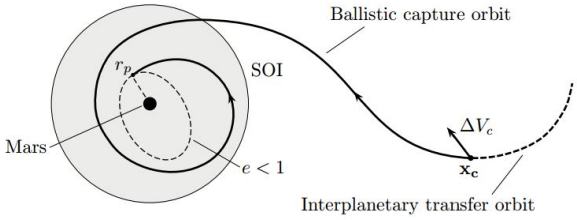

(c) Ballistic capture mechanism. Image source [8]

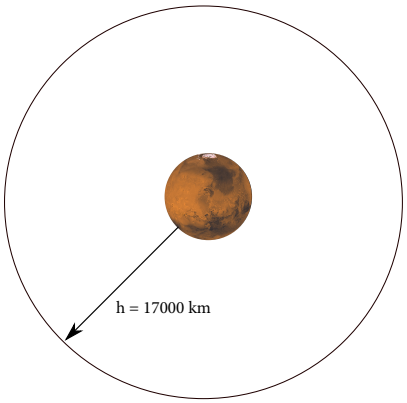

(d) Areosynchronous orbit at 17,000 km altitude

Figure 1: MARIO Mission Phases. In Fig (b), times t_d, t_f, and t_0 mark the beginning of heliocentric transfer & deep-space cruise, reaching of optimal conditions for ballistic capture, and the reaching of the first periapsis at Mars.

strategies could be used: a) time-optimal continuous thrusting or b) fuel-optimal bang-bang thrusting control. The critical resource for the electric propulsion system is the available power, since the specific impulse and thrust depend upon it. The selection of the thruster type is crucial.

At the end of the cruise, the spacecraft enters the Martian orbit through *Ballistic capture* (Fig. 1c). It is a phenomenon through which the spacecraft is *captured* when its Kepler energy becomes negative with respect to Mars only by the virtue of the natural gravitational forces between the Earth, Mars, and Sun [8, 35]. This is essentially a very low ΔV operation. Since the capture is achieved solely by the natural gravitational forces, it can also escape using the same mechanism, thus making it temporary. Overall, this requires substantially less ΔV compared to classic Hohmann transfers [8]. This is an ideal option for CubeSats, where a low control authority prevents performing a high-thrust burn at Mars arrival. Finally, a circularisation manoeuvre is pursued to enter an areosynchronous orbit that is 17,000 km from Martian surface for performing Radiation Imaging.

The simplified CONOPS for MARIO Mission is as follows:

1. CubeSat separation and injection into SSGTO
2. Commissioning, communication, de-tumbling and Solar Array deployment
3. Chemical thruster firing for orbit raising and Earth escape
4. Electric thruster firing for low-thrust transfer and autonomous deep-space cruise
5. Ballistic capture at Mars and circularisation to areosynchronous orbit
6. Science observation
7. Spacecraft disposal

The total mission lifetime is approximately 5 years, from Launch to Disposal. The science observations shall take place for 6 months. The total transfer is approximately 4.5 years. Crucial environmental factors severely affect the mission.

3. CHEMICAL PROPULSION

The chemical propulsion system for the MARIO mission is sized and designed based on critical requirements pertaining to ΔV, maximum thrust, burn time, mass, and safety. Additionally, the destabilising angular momentum produced by thrust misalignment plays a crucial role in determining the limitation of thrust and thrusting duration. The requirements for the chemical propulsion system are listed in Tab. 1

Table 1: Chemical Propulsion System Requirements

ID	Type	Requirement
CPROP-01	PER	The chemical propulsion system shall provide a minimum **ΔV = 450 m/s** for orbital transfer manoeuvres.
CPROP-02	PER	The chemical propulsion system shall have a maximum thrust of **3 N**
CPROP-03	PER	The maximum thrusting time of the chemical propulsion system shall be **600 seconds** per orbital manoeuvre
CPROP-04	CON	The total mass of the chemical propulsion system shall be no more than **7.5 kg**.
CPROP-05	CON	The chemical propulsion system shall utilise non-toxic propellants

The rationale for CPROP-01 is that the ΔV listed is the required value, including a 25% margin, to execute orbit raising manoeuvres for Earth escape starting from the initial SSGTO and to perform contingency manoeuvres if required. Requirement CPROP-02 puts a limitation on maximum thrust to control the destabilising momentum due to thrust misalignment. Maximum burning time is listed as a requirement in CPROP-03 to minimise gravity losses and destabilisation. Maximum mass (CPROP-04) of the chemical propulsion system is capped at 25% of the total spacecraft mass. Finally, as CPROP-05 states, non-toxic propellants need to be used to prevent internal and external contamination. The types PER and CON refer to performance and constraint, respectively.

The initial orbital elements considered for the injection orbit are semi-major axis, eccentricity, inclination, true anomaly, argument of perigee, and right ascension of the ascending node [a, e, i, θ, ω, Ω] = [51526 km, 0.8705, 0.01°, 0°, 0°, 0°], with perigee $h_p = 295$ km and apogee $h_a = 90000$ km. The required escape velocity at h_p is 10.931 km/s, considering the Earth's radius to be 6378 km. Since the initial velocity at perigee, v_{pi} = 10.57 km/s, the required ΔV for escape is $\sim$ 360 m/s.

The chemical propulsion system needs to fire at perigee point with a specific thrust for a specific duration. These two parameters, thrust T and burn time t_b, need to be determined. To simplify the problem, t_b is considered constant for every orbit raising manoeuvre, except the final manoeuvre which injects the spacecraft at a parabolic trajectory with $v_\infty = 0$ m/s. This value is slightly lower than the constant burn time value. For different specific impulse, I_{sp}, values, the $T - t_b$ combination could be different *.

A parametric analysis is done to calculate the total time for Earth escape through orbit raising and the required propellant mass for the operations. For a nested series of specific impulses ranging from 200 to 400 seconds, thrusts from 2 to 3 N, and burn times from 400 to 600 seconds, the total transfer times and the propellant masses are calculated for each set of $\{I_{sp}, T, t_b\}$.

The required propellant mass, $m_{p,b}$, for each burn is calculated using Eq. 1. The value of gravitational acceleration, g, is assumed to be 9.81 $\mathrm{m/s^2}$

$$m_{p,b} = \frac{T \cdot t_b}{I_{sp} \cdot g} \tag{1}$$

The total propellant mass is then $m_{p,ch} = m_{p,b} \times$ No. of burns. The acquired ΔV for each burn, denoted as ΔV_b is then calculated using Eq. 2. The wet mass of the spacecraft before each impulse is denoted by $m_{i,b}$.

$$\Delta V_b = -I_{sp} \cdot g \cdot \ln\left(1 - \frac{m_{p,b}}{m_{i,b}}\right) \tag{2}$$

The ΔV_b adds to the perigee velocity v_p after each manoeuvre and the apogee keeps increasing. The gravity loss is neglected in this calculation but could be as much as 5% of the overall ΔV. The orbit raising manoeuvres continue until the required ΔV = 360 m/s is reached, i.e., when perigee velocity v_p reaches escape velocity v_{esc} at r_p = 6673 km. Propellant mass m_p and minimum transfer period (for each thrust-burntime combination) are plotted as a function of I_{sp} in Fig. 2.

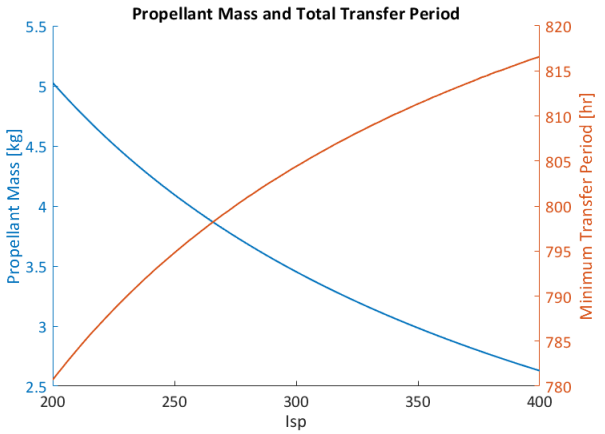

Figure 2: Propellant Mass and Minimum Transfer Period (for each $T - t_b$ combination) as a function of I_{sp}

*All thrust and specific impulse values used in this work pertain to vacuum conditions.

The transfer period is defined as the time period from initial orbit injection to Earth escape. The propellant mass decreases with the increase in I_{sp} whereas the transfer period increases. Depending upon the mission and system requirements, one could choose an I_{sp} design point such that the propellant mass is low or the transfer time is low. The design choice related to I_{sp} impose the choice of thrusters. Options such as cold gas and warm gas thrusters could be eliminated directly since they do not satisfy the requirements on thrust (< 1 N), maximum mass (> 8 kg), and specific impulse (< 100 s) to provide the required ΔV [2]. Monopropellant thrusters based on the blends of ammonium dinitramide (ADN) [36, 37] could be used since that satisfies the safety requirement CPROP-05. Bipropellant thrusters utilising hydrogen peroxide (H_2O_2) and ethanol (C_2H_5OH) also satisfy CPROP-05 [11]. The choice of the propulsion system is crucial since the capabilities of Monopropellant and Bipropellant systems are significantly different. For example, depending upon the fuel characteristics, the Monopropellant system has an I_{sp} of 260 s and the Bipropellant system has an I_{sp} of 315 s [11, 37].

From Fig. 3, the $T - t_b$ combination is picked from the zone where the transfer period is minimum (top-right).

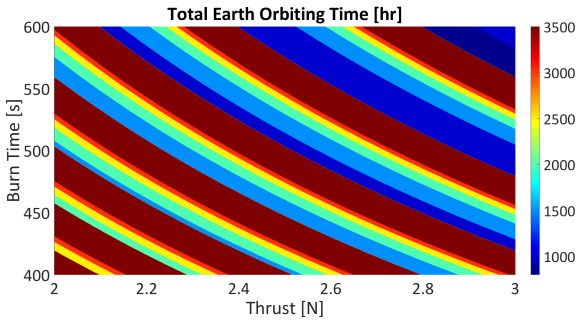

(a) Transfer Period [hr] for I_{sp} = 260 s

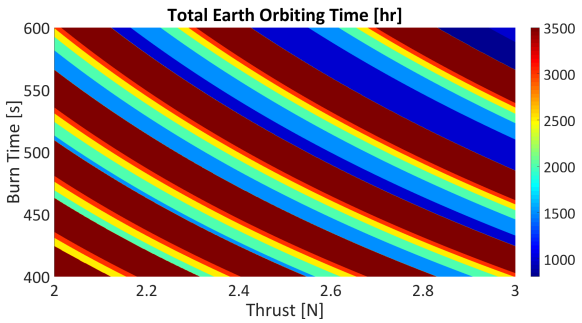

(b) Transfer Period [hr] for I_{sp} = 315 s

Figure 3: Total transfer period in hours as a function of Thrust and Burn time for Monopropellant (I_{sp} = 260 s) and Bipropellant thrusters (I_{sp} = 315 s)

For I_{sp} = 260 s: Thrust T = 2.91 N, burn time t_b = 576 s, propellant mass m_p = 3.947 kg, and the minimum transfer period P = 797 hours. For I_{sp} = 315 s: T = 2.926 N, t_b = 580.4 s, m_p = 3.297 kg, and P = 807 hours. In each case, the total number of orbital manouevres is 7 (6 raisings and 1 escape) and the amount of Van Allen Belt crossings is 13 (for each, inner and outer). Fig. 4 illustrates the orbit raising and Earth escape manoeuvres (I_{sp} = 260 s).

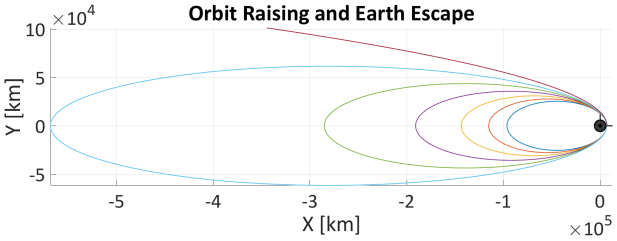

Figure 4: Orbit raising and Earth escape

The chemical system sizing is done by placing a 25% margin on the ΔV, which is a typical margin applied for low-maturity systems and this also accounts for gravity losses. Thus, the overall ΔV requirement rises to 450 m/s. The chemical propellant mass becomes 4.852 kg if the I_{sp} = 260 s and 4.065 kg if I_{sp} = 315 s.

3.1 Monopropellant thruster

The ADN-blend propellant, in Monopropellant thrusters, has a liquid phase density of 1290 $\mathrm{kg/m^3}$ [38]. Achievable specific impulse using ADN-based propellants is 230 - 260 s. In comparison, the widely used classic Monopropellant, Hydrazine, has 1020 $\mathrm{kg/m^3}$. The analysis is performed with I_{sp} = 260 s. Considering the margined propellant mass, 4.852 kg, the total propellant volume is 3761 $\mathrm{cm^3}$ or 3.761 litres, which in terms of CubeSat units is ∼3.8 U. A pressurised propellant tank containing 3.761 litres requires a spherical or a cylindrical shape for safety reasons. However, in a 16U CubeSat, it cannot be accommodated due to space and shape constraints, as a spherical tank would be of $\sim$ 9.65 cm radius.

To have a minimum volume of the tank while maintaining the pressure and to accommodate within the structure, dome-shaped cylindrical tanks known as *Cassini* tanks have to developed [39]. Since one large tank would be infeasible, four smaller Cassini tanks are proposed, each with 1.05 litre capacity including a $\sim$ 12% ullage volume. The radius of each tank is 4.7 cm and the height is 16.9 cm, thereby occupying $\sim$ 1.7 U space. Fig. 5 illustrates the shape and placement of the tanks in the spacecraft structure. Tank pressurisation has to be achieved using Gaseous N_2 or by sublimating a solid plate of CO_2.

To achieve the necessary thrust, either a large 3 N thruster or two 1.5 N thrusters could be used. Nozzle area ratio and the tank pressure influence the thrust level. The tank thickness is determined by tank pressure, $\sim$ 28 bar [40]. Assuming a 20% margin on the tank pressure, the tank thickness is 0.22 mm. Considering the material to be Titanium Alloy with a density of 4500 $\mathrm{kg/m^3}$, the tank mass is 0.044

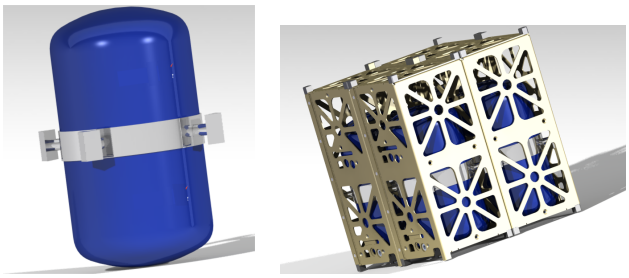

(a) Tank shape **(b)** Full structure

Figure 5: Monopropellant thruster tank shape and position inside the spacecraft structure [Courtesy: Mr. Sanz Casado]. Each tank occupies 1.7U

kg. The total mass of all four tanks is 0.176 kg. Tab. 2 summarises the characteristics of the Monopropellant chemical propulsion system. The overall mass of the Monopropellant propulsion system is 6.1 kg.

Table 2: Monopropellant chemical propulsion characteristics

Parameter	**Value**
Initial Mass, m_i	30 kg
Total Thrust, T	2.91 N
Specific Impulse, I_{sp}	260 s
Burn Time per manoeuvre, t_b	576.6 s
Orbit raising manoeuvres	7
Total ΔV (no margin)	359.8 m/s
Total ΔV (w/ 25% margin)	450 m/s
Propellant mass, $m_{p,mp}$ (no margin)	3.9471 kg
Propellant mass (w/ margin)	4.852 kg
Final Mass, $m_{final,mp}$	25.148 kg
Propellant density, ρ_p	1290 $\mathrm{kg/m^3}$
Propellant volume, V_p	3761 $\mathrm{cm^3}$
Ullage vol % per tank	12 %
Tank volume (each), V_{tank}	1053 $\mathrm{cm^3}$
No. of tanks	4
Tank radius, R_{tk}	4.7 cm
Tank height, H_{tk}	16.9 cm
Tank thickness, W_{tk}	0.22 mm
Material density, ρ_{tk}	4500 $\mathrm{kg/m^3}$
Tank mass (each), m_{tk}	0.062 kg
Tank mass (total)	0.248 kg
Thruster mass, m_T	0.6 kg
Pressurisation system mass, m_{pr}	0.3 kg
Feed system mass, m_{fs}	0.1 kg
Total mass	6.1 kg

3.2 Bipropellant thruster

Bipropellant thrusters that use ethanol ($\rho = 789$ $\mathrm{kg/m^3}$) and hydrogen peroxide ($\rho = 1450$ $\mathrm{kg/m^3}$) provide a higher thrust and have a high specific impulse than Monopropellant thrusters [10, 11]. Usage of H_2O_2 is advantageous for two reasons, a) it is non-toxic and its filling is considered non-hazardous, and b) it is a self-pressurising. Bipropellant thrusters have not been developed for CubeSats yet due to their high complexity, although they would reduce the overall mass of the propulsion system. The feed system can be either pressure fed or pump fed. In the latter case, microturbines and micropumps should be used to feed the propellants into the combustion chamber [41], which will lead to the reduction of tank pressure and subsequently the tank size. Ethanol is directly fed into the chamber while H_2O_2 passes through a catalyst bed (typically a monolithic structure made of mullite and coated with alumina [11, 41]) and decomposes into H_2O and O_2. The exothermic nature of the reaction converts the catalyst to a gaseous form which drives the microturbines that power the pumps. The O_2/H_2O mixture then passes through the cooling channels that surround the nozzle, throat, thrust chamber, and is finally injected into the thrust chamber at a certain mixture ratio with ethanol for ignition and combustion [11].

Table 3: Bipropellant chemical propulsion characteristics

Parameter	**Value**
Initial Mass, m_i	30 kg
Total Thrust, T	2.926 N
Specific Impulse, I_{sp}	315 s
Burn Time per manoeuvre, t_b	580.4 s
Orbit raising manoeuvres	7
Total ΔV (no margin)	359.8 m/s
Total ΔV (w/ 25% margin)	450 m/s
Propellant mass, $m_{p,bp}$ (no margin)	3.297 kg
Propellant mass (w/ margin)	4.065 kg
Final Mass, $m_{final,bp}$	25.935 kg
Mass Mixture Ratio(O/F)	4.5
Fuel Mass, m_F	0.739 kg
Oxidiser Mass, m_{OX}	3.326
Fuel density, ρ_F	789 $\mathrm{kg/m^3}$
Oxidiser density, ρ_{OX}	1450 $\mathrm{kg/m^3}$
Fuel volume, V_F	936.6 $\mathrm{cm^3}$
Oxidiser volume, V_{OX}	2293.8 $\mathrm{cm^3}$
Ullage vol % per tank	10 %
Fuel tank volume, $V_{tk,F}$	1030 $\mathrm{cm^3}$
Oxidiser tank volume, $V_{tk,OX}$	3×841 $\mathrm{cm^3}$
No. of tanks	4
Tank radius, R_{tk}	4.7 cm
Tank thickness, W_{tk}	0.1 mm
Fuel tank height, $H_{tk,F}$	15 cm
Oxidiser tank height, $H_{tk,F}$	12.2 cm
Material density, ρ_{tk}	4500 $\mathrm{kg/m^3}$
Fuel tank mass, $m_{tk,F}$	0.0226 kg
Oxidiser tank mass, $m_{tk,OX}$	3×0.0162 kg
Total tank mass, $m_{tk,tot}$	0.06 kg
Thruster mass, m_T	0.2 kg
Feed system mass, m_{fs}	0.5 kg
Total mass	4.8 kg

The total propellant mass required is 4.065 kg including

the margin. Assuming a mass mixture ratio (O/F) of 4.5, the mass of the oxidiser H_2O_2 is 3.326 kg and the mass of the fuel C_2H_5OH is 0.739 kg. Considering the densities, the oxidiser volume, V_{OX} is 2.293 litres and the fuel volume, V_F is 0.936 litres. The overall propellant volume is 3.23 litres. The oxidiser can be stored in three 0.84 litre titanium-alloy tanks while the fuel can be stored in one 1.03 litre tank [42], overall 4 tanks. The radius of all tanks is kept at 4.7 cm while the heights of oxidiser and fuel tanks are 12.2 cm and 15 cm, respectively. Since the tank pressurisation is lower than that of the Monopropellant tanks, the tank thickness is ~ 0.1 mm. The overall tank mass is 0.06 kg. The thruster, microturbine, and the micropump weigh 0.7 kg. The overall mass of the propulsion system is < 5 kg. The Bipropellant chemical propulsion characteristics are listed in Tab. 3.

Table 4: Comparison between Monopropellant and Bipropellant systems

Criteria→ / Options↓	Thrust [N]	Isp [s]	Mass [kg]	Vol [U]	Complexity
Monoprop	3	~ 260	$\sim$6	8	Medium
Biprop	3	~ 315	$\sim$5	6	High

The main advantage of Monopropellant system is its relative simplicity in comparison with Bipropellant systems. CubeSat Bipropellant systems need further development. However, the specific impulse and thrusting capabilities of Bipropellant systems are far superior to those of the Monopropellant systems. Combustion chamber thermal radiation emission is another issue that affects the mission. Bipropellant systems have a chamber temperature ~ 3000 K whereas for Monopropellant systems it is ~ 2000 K [43]. The overall mass & transfer times for Monopropellant and Bipropellant systems are 6.1 kg & 797 hours and 4.8 kg & 807 hours, respectively.

4. ELECTRIC PROPULSION

Once Earth escape is achieved using the chemical propulsion system, the deep-space cruise phase starts. The cruise lasts for ~ 4.4 years and culminates in ballistic capture [8]. Electric propulsion system, which has high I_{sp}, is utilised to enable the cruise and ballistic capture. The environmental conditions encountered in the heliocentric phase significantly affect the mission. Firstly, as the distance between the spacecraft and the Sun increases, the power generation capability decreases since the Solar constant decreases by $1/r^2$, with r being the Sun-S/C distance. Additionally, Solar Radiation Pressure causes perturbation of the cruise trajectory.

Transfer to Mars after Earth escape could be achieved by two techniques, a time-optimal solution where the thruster continuously thrusts, thereby minimising the transfer time and a fuel-optimal solution where the thruster fires intermittently to control the trajectory while minimising fuel consumption; this is otherwise known as the bang-bang control. The ΔV accumulated over the cruise varies significantly based on the transfer technique that is utilised. Depending upon the mission and system requirements, one could choose the technique that suits. The requirements of the electric propulsion system are listed in Tab. 5.

Table 5: Electric Propulsion System Requirements

ID	Type	Requirement
EPROP-01	PER	The maximum transfer time shall be **4.5 years** for cruise and ballistic capture.
EPROP-02	PER	The electric propulsion system shall have a maximum power consumption of **60 W**
EPROP-03	CON	The total mass of the electric propulsion system shall be no more than **7.5 kg**.

The rationale for EPROP-01 is to constrain the maximum transfer time such that valuable science products can be obtained before the end of the mission lifetime, ~ 5 years. Since the power availability for the thruster is critical, EPROP-02 imposes a maximum limit on the power consumption of the thruster. The maximum allowable mass of the electric propulsion system, including the propellant and the components, is set at $\sim 25\%$ of the overall spacecraft mass.

The choice of the electric propulsion system is very crucial. The options are electrothermal, electrostatic, and electromagnetic thrusters. Since high I_{sp} values are required and subsequently high firing times are envisaged, electrostatic thrusters like the Gridded Ion Thrusters are a suitable choice. Gridded Ion Thrusters applicable for Interplanetary CubeSats have an I_{sp} in the range of 1500-3500 seconds and a propulsion lifetime in the order of 30,000 hours [18, 29]. Another suitable option would be the Hall Effect Thruster, which compared to a Gridded Ion Thruster, has a lower specific impulse but higher thrust for the same input power. Electromagnetic thruster options such as Pulsed Plasma Thrusters (PPTs) and Magnetoplasmadynamic (MPD) thrusters have lifetimes and thrust-to-power ratios that are very low [29]. Helicon thrusters are promising candidates but their low efficiency and lifetime pose a problem. Tab. 6 compares the different electric thruster types applicable for CubeSats [2, 25, 29, 44, 45].

Table 6: Comparison of electric propulsion options

Type	Thrust [mN]	I_{sp} [s]	Power [W]	Life [hr]
Ion	0.5-1.4	1500-3500	30-80	30000
Hall	1.8-4	800-1400	60-120	10000
PPT	0.01-1	500-1500	10-30	1000
Helicon	0.8-1.5	900-1200	50-80	1000

Considering the high thruster lifetime, specific impulse, and power consumption requirements, the Gridded Ion Thruster is chosen for the analysis (illustration Fig. 6).

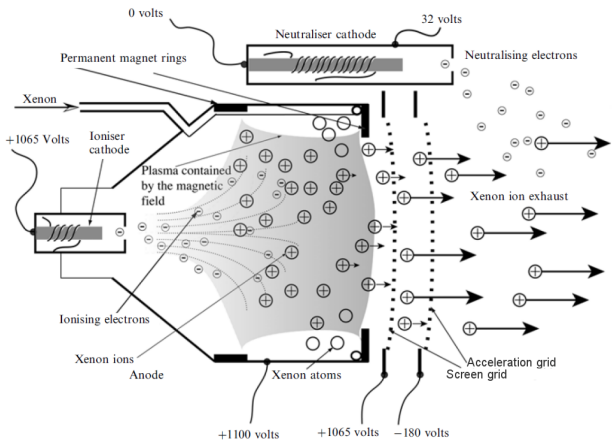

Figure 6: Illustration of NSTAR Ion Thruster [46]

Both thrust and I_{sp} vary with varying thruster input power P_{in}, which in turn is a fraction of the overall available power to the system. The power available to the electric propulsion system is calculated as a function of the distance between the spacecraft and the Sun. Fig.7 illustrates the available and consumed power. The 60 W limit on Fig. 7 is due to the requirement EPROP-02. The total power generated at BOL (at Earth) is 137 W and at EOL (at Mars) it is 57 W. A distribution efficiency of 85% is considered and the power available to the subsystems is reduced to 116.5 W and 49 W at BOL and EOL respectively. During the transfer, apart from the thruster, critical subsystems such as the On-Board Computer, ADCS, and the Electrical Power System are always active while other subsystems are operated when required. Rest of the subsystems consume 24.2 W to 18.4 W depending upon the operations and power availability. As the distance increases, the power available to the thruster reduces from 60 W limit to 30.56 W.

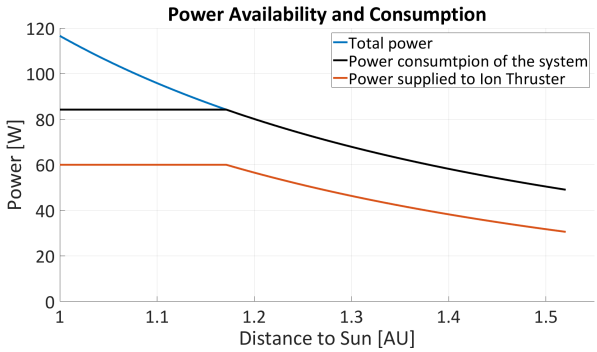

Figure 7: Available and consumed power as a function of the Sun-S/C distance

The thruster characteristics are defined based on the current state of the art, the Iodine-fueled BIT-3 mini RF Ion Thruster [44]. The maximum thrust is 1.34 mN and maximum I_{sp} is 3251 seconds. Nominally, Xenon is used as the propellant for RF Ion Thrusters due to its high molecular mass, 131.2 kg/kmol. Although it has many advantages, storability of Xenon in cryogenic state inside a high pressure tank makes the thermal control system and the structure untenable in a CubeSat. Thus, Iodine is chosen as the propellant because a) it has a molecular mass of 126.9 kg/kmol which is similar to that of Xenon, b) it can be stored in a solid form at room temperature and then sublimated using a low-power heat source, and c) the storage tank size and mass are greatly reduced due to its high density and very low pressurisation (< 50 Pa) is required. The potential problem associated with Iodine is its ability to corrode the components. However, this can be prevented by utilising corrosion-resistant ceramic materials for plasma-chamber walls [18]. Power distribution and regulation to the thruster is achieved using Power Processing and Control Units (PPCUs). The thruster characteristics are listed in Tab. 7.

Table 7: Electric thruster characteristics

Parameters	**Value**
Type	RF Ion Thruster
Propellant	Iodine
Molecular Mass, $\mathfrak{M}$	126.9 $\mathrm{kg/kmol}$
Prop. Density, ρ_p	4930 $\mathrm{kg/m^3}$
Max Thrust, T_{max}	1.34 mN
Max I_{sp}	3251 s
Max Power, P_{max}	60 W
Prop. Flow Rate, $\dot{m}_p$,	42 μg/s
Thruster Efficiency, η_T	0.36
Electrical Efficiency, η_e	0.59
Mass Utilisation Efficiency, η_m	0.61
Beam Voltage, V_b	1900 V
PPCU mass, m_{PPCU}	0.5 kg
Thruster mass, m_T	0.1 kg

The propellant flow rate is fixed at 42 $\mu g/s$ and the beam voltage, V_b, which is the potential difference between the screen grid and the acceleration grid is 1900 V, with $V_{screen} = 1800$ V and $V_{acc} = -100$ V (negatively biased to the spacecraft). The mass utilisation efficiency, η_m is the ratio of ion mass flow rate $\dot{m}_i$ and propellant mass flow rate $\dot{m}_p$. Experimental analysis of the BIT-3 using Iodine yields 61% mass utilisation efficiency [44]. The thruster electrical efficiency or the energy efficiency, η_e is 59%. The total thrust efficiency η_T, which is the product of mass utilisation and electrical efficiencies, is 36%.

The thrust and I_{sp} variation with the input power are calculated using the electrostatic propulsion principles. Considering singly charged ions of Iodine (without double-charging), the thrust is expressed using Eq. 3 where, e is the electric charge per kmol of electrons (Faraday constant) with a value 96485332.89 $\mathrm{C\,kmol^{-1}}$. The quantity I_b is the beam current. This is determined by calculating the beam power P_b from the input power P_{in} and electrical efficiency η_e. These are expressed in Eq. 4 [47].

$$T = \sqrt{\frac{2\,\mathfrak{M}}{e}}\; I_b\; \sqrt{V_b} \tag{3}$$

$$\eta_e = \frac{P_b}{P_{in}} \qquad I_b = \frac{P_b}{V_b} \tag{4}$$

The specific impulse variation is expressed using Eq. 5

$$I_{sp} = \sqrt{\frac{2\,\mathfrak{M}\,V_b}{e}} \cdot \frac{I_b}{\dot{m}_p\, g_0} = \frac{T}{\dot{m}_p\, g_0} \tag{5}$$

The thrust and specific impulse variation as a function of the input power is illustrated in Fig. 8. The relationship is linear and the parameters decrease with decreasing input power.

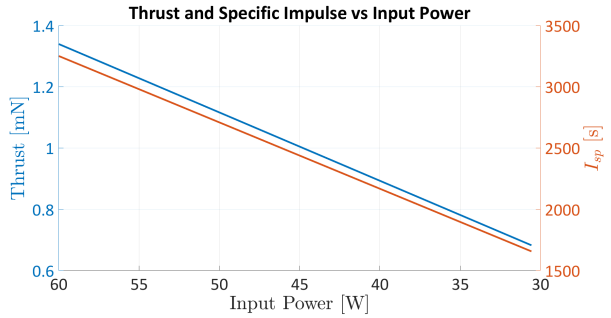

Figure 8: Variation of thrust and specific impulse with input power

Utilising the information on thruster characteristics, an optimal control problem considering the spacecraft dynamics and real Solar System dynamics, including that of Solar Radiation Pressure and Low-Thrust Trajectory Control is solved to compute the transfer trajectory. The initial mass of the spacecraft after Earth escape is 25.935 kg (see Tab. 3). The constraints of the optimal control problem are input power $P_{in} \in [60, 30.56]$ W, thrust $T \in [1.34, 0.68]$ N, and specific impulse $I_{sp} \in [3251, 1656]$ seconds. The boundary conditions are set for departure (beginning of cruise) and arrival at Mars. The departure boundary conditions are initial mass (25.935 kg) and direction of the spacecraft. The arrival boundary condition includes any state (position and velocity) corresponding to the ballistic capture trajectory requirement. These are retrieved from splines computed using a modified version of the MATLAB tool called "GRATIS" [31, 48]. Cost functions are defined to obtain a time-optimal and a fuel-optimal solutions. The optimal control problem is solved using a Direct Method, in which it undergoes a direct transcription [31, 49].

The simulations are performed in the *Radial-Tangential-Normal* (RTN) frame, starting from epoch t_0 (which in this case is the time of departure t_d). The spacecraft states and the thrust orientations are defined in *Spacecraft-Radial-Tangential-Normal* (SRTN) frame (illustrated in Fig. 9). The axis +r is aligned with the Mars-Spacecraft line and it points in the direction opposite to the planet and towards the spacecraft. The axis +ϕ is aligned with the angular momentum

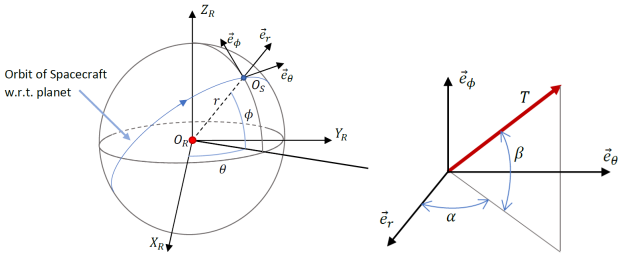

(a) SRTN frame **(b)** Thrust orientation

Figure 9: Spacecraft-Radial-Tangential-Normal frame and the thrust orinetation.

vector of the spacecraft w.r.t to Mars. The axis +θ completes the right-handed frame. The angles α and β represent the azimuth and zenith angles respectively in the spacecraft body frame.

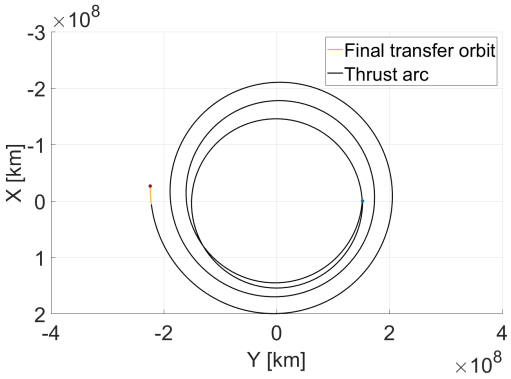

(a) Trajectory

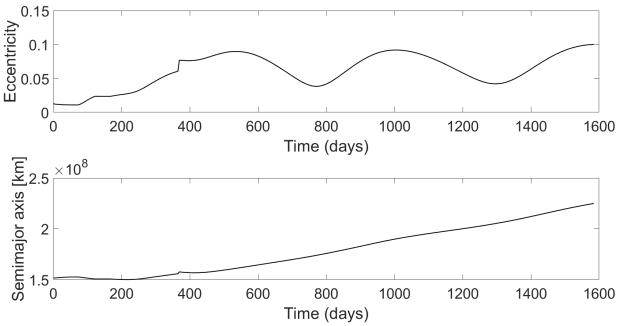

(b) Orbital elements

Figure 10: Spacecraft trajectory, eccentricity and semi-major axis variation in time-optimal solution.

The time-optimal problem yields a total transfer time of 1584.38 days ($\sim$ 4.34 years), which satisfies EPROP-01. Since this is a long duration flight, the system components should have sufficient radiation protection to prevent failures. The overall propellant mass is 5.751 kg. The corresponding Iodine volume is 1166.6 cm^3. Since Iodine can be stored in solid state, the corresponding dimensions of the tank are 20 $\times$ 10 $\times$ 5.85 cm^3, with 3.4 cm^3 *ullage* volume for iodine

sublimation. The continuous thrust trajectory is illustrated in Fig. 10 and the profiles of T and I_{sp} during the transfer are illustrated in Fig. 11. The "overall ΔV" of the time-optimal solution is 6.91 km/s.

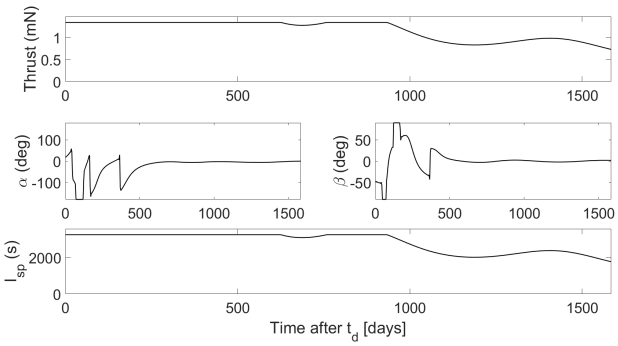

Figure 11: Thrust and I_{sp} profiles as a function of time in the time-optimal solution.

The fuel-optimal solution yields a transfer time of 1584.48 days (4.34 years) which also satisfies EPROP-01. The overall propellant mass is 5.745 kg, the propellant volume is 1165.3 cm^3, and the tank dimensions are 20 $\times$ 10 $\times$ 5.84 cm^3. The ΔV for all manouevres is 6.9 km/s and the difference between departure and arrival velocities is 4.854 km/s. The spacecraft eccentricity and semi-major axis are illustrated in Fig. 12. The profiles of T and I_{sp} are illustrated in Fig. 13. It has to be noted that as a stringent and short constraint on overall transfer time is placed, the fuel-optimal solution tends towards time-optimal solution as the transfer has to be achieved within the given period. Departure-arrival time of flight window requirement needs to be relaxed to appreciate the difference. Time-optimal strategies are better for short windows and fuel-optimal strategies are better for long windows.

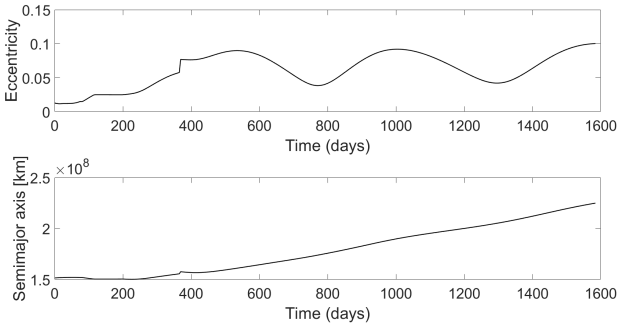

Figure 12: Semi-major axis and eccentricity variation in fuel-optimal solution.

Once ballistic capture is achieved, free revolutions are obtained and the spacecraft stays in highly eccentric orbits for a period of 6 months to 1 year. Dynamics are very unstable and careful manoeuvre planning has to be done. Circularisation at 17,000 km altitude orbit consumes significant

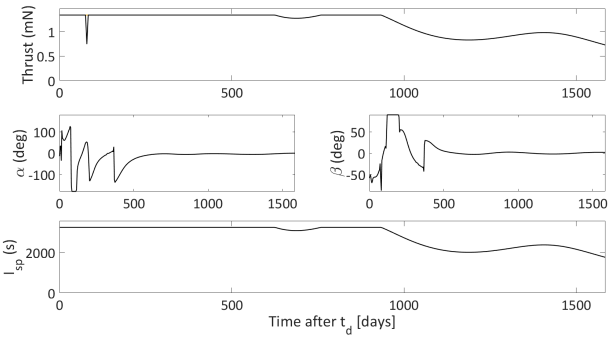

Figure 13: Thrust and I_{sp} profiles as a function of time in the fuel-optimal solution.

resources since the eccentricity (>0.9) of the initial injection orbit is very high. Instantaneous manoeuvres require $\Delta V \sim 0.95$ km/s. Performing a short-duration high-thrust braking manoeuvre that provides ΔV = 60 m/s (accounted in the chemical propulsion margin) and circularising using low-thrust propulsion to 17,000 km requires m_p = 1.73 kg and ΔV = 1.104 km/s. Circularisation at 60,000 km requires m_p = 1.25 kg and ΔV = 0.79 km/s. A trade-off needs to be performed, taking into account the payload observation capabilities. Optimisation of low-thrust circularisation is currently being pursued by including the ballistic capture dynamics to yield a lower propellant mass and to improve accuracy.

5. DUAL PROPULSION

The concept of dual propulsion is game changer for interplanetary CubeSat and microsatellite missions. Traditionally, interplanetary satellites have mainly used the chemical propulsion system. Some missions have utilised the electric propulsion system. Sole usage of chemical propulsion will lead to very large propellant mass and a very low transfer time. Sole usage of electric propulsion will lead to very large transfer time but with considerably low propellant mass. No mission up to date has utilised both the systems for primary propulsion. The idea behind this work was to balance the two quantities and arrive at a solution where the interplanetary mission could be achieved from an Earth-based orbit to Mars with a reasonable propellant mass and transfer time.

Table 8: Dual propulsion characteristics

Parameter	Chemical	Electric
Flight Time [days]	33.625	1584.48
Prop. Mass [kg]	4.065	5.745†
Sys. Mass (wet) [kg]	4.8	6.245†
Size [U]	6	1.5
ΔV [km/s]	0.36	6.9†
Peak Power [W]	24	60

† Fuel optimal-solution used. Does not include circularisation m_p and ΔV.

The dual propulsion characteristics are listed in Tab. 8. The chemical propulsion weighs $\sim$16% of the total spacecraft mass while the electric propulsion weighs $\sim$21%. The percentage volume occupied by the chemical and electric systems are 37.5% and 9.4% respectively. Both systems are crucial for the achieving the mission since the chemical stage reduces the transfer time and the electric stage reduces the required propellant mass.

6. CONCLUSION

This work set out to analyse the dual chemical-electric propulsion concept for stand-alone interplanetary CubeSat missions. The emphasis is on the word *dual*, since the chemical propulsion and electric propulsion are two different systems in the same satellite used in different mission phases. The chemical stage enables swift Earth escape through a series of orbit raising manoeuvres while the electric stage enables deep-space cruise and ballistic capture. The overall transfer time and propellant mass are balanced to make the system and the mission feasible. Chemical propulsion weighs 4.8 kg, occupies 6U, and provides a ΔV of 450 m/s. The electric propulsion weighs 6.245 kg, occupies 1.5 U, and provides a ΔV of 6.9 km/s. Future work entails a combined trajectory optimisation for cruise, capture and circularisation. Detailed design of the two propulsion systems is currently being pursued.

ACKNOWLEDGEMENT

This work was pursued as a collaborative effort between Politecnico di Milano, Italy and Delft University of Technology, the Netherlands. Special thanks to the PhD school of Politecnico for providing the IDEA League Research Grant. The authors would like to expressly Mr. Alvaro Sanz Casado and Mr. Goncalo Cruz Chambel de Aguiar whose MSc theses at Politecnico di Milano and TU Delft, respectively, were immensely helpful for this work. The authors are also greatly thankful for the contributions of Mr. Fernando Soler Lanagran of Politecnico di Milano & Universidad de Sevilla.

REFERENCES

[1] T. H. Zurbuchen, R. von Steiger, S. Bartalev, X. Dong, M. Falanga, R. Fléron, A. Gregorio, T. S. Horbury, D. Klumpar, M. Küppers *et al.*, "Performing high-quality science on cubesats," *Space Research Today*, vol. 196, pp. 11–30, 2016.

[2] K. Lemmer, "Propulsion for cubesats," *Acta Astronautica*, vol. 134, pp. 231–243, 2017.

[3] G. Manzoni, "Design of a highly integrated micropropulsion system for microsatellites attitude control," in *36th AIAA/ASME/SAE/ASEE Joint Propulsion Conference and Exhibit*, 2000, p. 3476.

[4] R. Staehle, D. Blaney, H. Hemmati, M. Lo, P. Mouroulis, P. Pingree, T. Wilson, J. Puig-Suari, A. Williams, B. Betts *et al.*, "Interplanetary cubesats: opening the solar system to a broad community at lower cost," *Journal of small satellites*, vol. 2, no. 1, pp. 161–186, 2013.

[5] R. Walker, D. Kochny, C. Bramanti, and I. Carnelli, "Miniaturised Asteroid Remote Geophysical Observer (M-ARGO): a stand-alone deep space cubesat system for low-cost science and exploration missions," in *6th Interplanetary CubeSat Workshop - Cambridge*. iCubeSat, 2017. [Online]. Available: https://icubesat.files.wordpress.com/2017/05/2017-a-3-1-20170530134557-m-argo.pdf

[6] A. Klesh and J. Krajewski, "Marco: Cubesats to mars in 2016," in *Proceedings of the 29th Annual AIAA/USU Small Satellite Conference: SSC15-III-3*, 2015.

[7] S. Asmar and S. Matousek, "Mars Cube One (MarCO): the first planetary cubesat mission," in *Proceedings of the Mars CubeSat/NanoSat Workshop, Pasadena, California, November*, vol. 20, 2014, p. 21.

[8] F. Topputo and E. Belbruno, "Earth–mars transfers with ballistic capture," *Celestial Mechanics and Dynamical Astronomy*, vol. 121, no. 4, pp. 329–346, 2015.

[9] C. Scharlemann, M. Schiebl, K. Marhold, M. Tajmar, P. Miotti, C. Kappenstein, Y. Batonneau, R. Brahmi, and C. Hunter, "Development and test of a miniature hydrogen peroxide monopropellant thruster," in *42nd AIAA/ASME/SAE/ASEE Joint Propulsion Conference & Exhibit*, 2006, p. 4550.

[10] D. Scharfe and A. Ketsdever, "A review of high thrust, high delta-v options for microsatellite missions," in *45th AIAA/ASME/SAE/ASEE Joint Propulsion Conference & Exhibit*, 2009, p. 4824.

[11] C. Scharlemann and M. Tajmar, "Development of propulsion means for microsatellites," in *43rd AIAA/ASME/SAE/ASEE Joint Propulsion Conference & Exhibit*, 2007, p. 5184.

[12] H. Barber, C. Buell, G. Falkenstein, and R. Gurnitz, "Microthrusters employing catalytically reacted n2-o2-h2 gas mixtures, tridyne," *Journal of Spacecraft and Rockets*, vol. 8, no. 2, pp. 111–116, 1971.

[13] J. Mueller, R. Hofer, and J. Ziemer, "Survey of propulsion technologies applicable to cubesats," in *Joint Army-Navy-NASA-Air Force (JANNAF), Colorado Springs, CO; United States*, 2010.

[14] M. M. Micci, *Micropropulsion for small spacecraft*. Aiaa, 2000, vol. 187.

[15] B. Reed, W. d, and L. Dang, "Experimental evaluation of cold flow micronozzles," in *37th Joint Propulsion Conference and Exhibit*, 2001, p. 3521.

[16] F. Maggi, G. Gariani, L. Galfetti, and L. T. DeLuca, "Theoretical analysis of hydrides in solid and hybrid rocket propulsion," *international journal of hydrogen energy*, vol. 37, no. 2, pp. 1760–1769, 2012.

[17] A. Ketsdever and J. Mueller, "Systems considerations and design options for microspacecraft propulsion systems," in *35th Joint Propulsion Conference and Exhibit*, 1999, p. 2723.

[18] M. Tsay, J. Frongillo, and J. Zwahlen, "Maturation of iodine fueled BIT-3 RF ion thruster and RF neutralizer," in *52nd AIAA/SAE/ASEE Joint Propulsion Conference*, 2016, p. 4544.

[19] N. Wells, R. Walker, S. Green, and A. Ball, "Simone: Interplanetary microsatellites for neo rendezvous missions," *Acta Astronautica*, vol. 59, no. 8-11, pp. 700–709, 2006.

[20] M. Berti, L. Biagioni, U. Cesari, M. Saverdi, and M. Andrenucci, "Development and preliminary characterization of a low power hall thruster prototype," in *40 th AIAA/ASME/SAE/ASEE Joint Propulsion Conference and Exhibit*, 2004.

[21] V. Khayms and M. Martinez-Sanchez, "Design of a miniaturized hall thruster for microsatellites," in *32nd Joint Propulsion Conference and Exhibit*, 1996, p. 3291.

[22] M. Tajmar, A. Genovese, and W. Steiger, "Indium field emission electric propulsion microthruster experimental characterization," *Journal of propulsion and power*, vol. 20, no. 2, pp. 211–218, 2004.

[23] C. D. Rayburn, M. E. Campbell, and A. T. Mattick, "Pulsed plasma thruster system for microsatellites," *Journal of spacecraft and rockets*, vol. 42, no. 1, pp. 161–170, 2005.

[24] M. Andrenucci, "Magnetoplasmadynamic thrusters," *Encyclopedia of Aerospace Engineering*, 2010.

[25] D. Pavarin, F. Ferri, M. Manente, D. Curreli, Y. Guclu, D. Melazzi, D. Rondini, S. Suman, J. Carlsson, C. Bramanti *et al.*, "Design of 50 w helicon plasma thruster," in *31st Int. Electric Propulsion Conf., Ann Arbor, MI*, 2009, pp. 2009–205.

[26] C. Charles, R. Boswell, P. Alexander, C. Costa, O. Sutherland, L. Pfitzner, R. Franzen, J. Kingwell, A. Parfitt, P.-E. Frigot *et al.*, "Helicon double layer thrusters," in *Proc. 27th Int. Conf. on Phenomena in Ionized Gases (Eindhoven: ICPIG), http://www. icpig2005. nl/cd/D:/Proceedings_ICPIG_2005. html*, 2005.

[27] A. Cervone, A. Mancas, and B. Zandbergen, "Conceptual design of a low-pressure micro-resistojet based on a sublimating solid propellant," *Acta Astronautica*, vol. 108, pp. 30–39, 2015.

[28] P. D´ Arrigo and S. Santandrea, "The apies microsatellite mission to explore the asteroid belt," in *Small Satellites, Systems and Services*, vol. 571, 2004.

[29] S. Mazouffre, "Electric propulsion for satellites and spacecraft: established technologies and novel approaches," *Plasma Sources Science and Technology*, vol. 25, no. 3, p. 033002, 2016.

[30] "SpaceX Falcon 9 Data Sheet - Space Launch Report," http://www.spacelaunchreport.com/falcon9ft.html, accessed: April 02, 2018.

[31] G. Cruz Chambel de Aguiar, "Earth–mars low-thrust transfers with ballistic capture and real-solar-system dynamics," Master's thesis, Delft University of Technology, 2017.

[32] T. Sweetser, R. Maddock, J. Johannesen, J. Bell, P. Penzo, A. Wolf, S. Williams, S. Matousek, and S. Weinstein, "Trajectory design for a europa orbitter mission: A plethora of astrodynamic challenges," 1997.

[33] V. Franzese, K. Mani, and F. Topputo, "Autonomous optical navigation for interplanetary cubesats," in *24th Conference of the Italian Association of Aeronautics and Astronautics (AIDAA 2017)*, 2017, pp. 1–8.

[34] V. Franzese, P. Di Lizia, and F. Topputo, "Autonomous optical navigation for lumio mission," in *2018 Space Flight Mechanics Meeting*, 2018, p. 1977.

[35] Z.-F. Luo, F. Topputo, F. Bernelli-Zazzera, and G.-J. Tang, "Constructing ballistic capture orbits in the real solar system model," *Celestial Mechanics and Dynamical Astronomy*, vol. 120, no. 4, pp. 433–450, 2014.

[36] K. Anflo and B. Crowe, "In-space demonstration of an adn-based propulsion system," in *47th AIAA/ASME/SAE/ASEE Joint Propulsion Conference & Exhibit*, 2011, p. 5832.

[37] A. S. Gohardani, J. Stanojev, A. Demairé, K. Anflo, M. Persson, N. Wingborg, and C. Nilsson, "Green space propulsion: Opportunities and prospects," *Progress in Aerospace Sciences*, vol. 71, pp. 128–149, 2014.

[38] T. Zhang, G. Li, Y. Yu, Z. Sun, M. Wang, and J. Chen, "Numerical simulation of ammonium dinitramide (adn)-based non-toxic aerospace propellant decomposition and combustion in a monopropellant thruster," *Energy Conversion and Management*, vol. 87, pp. 965–974, 2014.

[39] P. Enright and E. Wong, "Propellant slosh models for the cassini spacecraft," in *Astrodynamics Conference*, 1994, p. 3730.

[40] R. A. Spores, "GPIM AF-M315E propulsion system," in *51st AIAA/SAE/ASEE Joint Propulsion Conference*, 2015, p. 3753.

[41] C. Scharlemann, M. Schiebl, K. Marhold, M. Tajmar, P. Miotti, C. Guraya, F. Seco, C. Kappenstein, Y. Batonneau, R. Brahmi *et al.*, "Test of a turbo-pump fed miniature rocket engine," in *42nd AIAA/ASME/SAE/ASEE Joint Propulsion Conference & Exhibit*, 2006, p. 4551.

[42] V. Berenblim, L. Kharitonova, I. Yakushcheva, and Z. Zharikova, "The compatibility of titanium alloys with hydrogen peroxide solutions," Foreign Technology Div. Wright-Patterson AFB, Ohio, Tech. Rep., 1973.

[43] L. Werling, N. Perakis, B. Hochheimer, H. K. Ciezki, and S. Schlechtriem, "Experimental investigations based on a demonstrator unit to analyze the combustion process of a nitrous oxide/ethene premixed green bipropellant," in *5th CEAS Air & Space Conference*, vol. 7, no. 11, 2015.

[44] M. Tsay, J. Frongillo, and K. Hohman, "Iodine fueled mini rf ion thruster for cubesat applications," in *34th International Electric Propulsion Conference, Kobe, Japan*, 2015.

[45] W. Wright and P. Ferrer, "Electric micropropulsion systems," *Progress in Aerospace Sciences*, vol. 74, pp. 48–61, 2015.

[46] M. J. Turner, *Rocket and spacecraft propulsion: principles, practice and new developments*. Springer Science & Business Media, 2008.

[47] D. M. Goebel and I. Katz, *Fundamentals of electric propulsion: ion and Hall thrusters*. John Wiley & Sons, 2008, vol. 1.

[48] Z.-F. Luo and F. Topputo, "Capability of satellite-aided ballistic capture," *Communications in Nonlinear Science and Numerical Simulation*, vol. 48, pp. 211–223, 2017.

[49] F. Topputo and C. Zhang, "Survey of direct transcription for low-thrust space trajectory optimization with applications," in *Abstract and Applied Analysis*, vol. 2014. Hindawi, 2014.